



Article

Seed Micromorphology, *In Vitro* Germination, and Early-Stage Seedling Morphological Traits of *Cattleya purpurata* (Lindl. & Paxton) Van den Berg

Miriam Bazzicalupo ^{1,*}, Jacopo Calevo ^{2,*}, Martino Adamo ^{2,3}, Annalisa Giovannini ⁴, Andrea Copetta ⁴ and Laura Cornara ¹

¹ Department of Earth, Environment and Life Sciences, University of Genoa, Corso Europa 26, 16132 Genoa, Italy; laura.cornara@unige.it

² Department of Life Sciences and Systems Biology, University of Turin, Viale Mattioli 25, 10125 Turin, Italy; martino.adamo@unito.it

³ Ecologie Microbienne, UCBL, CNRS, INRA, University of Lyon 1, Boulevard du 11 Novembre 1918 43, 69622 Villeurbanne, France

⁴ CREA Research Centre for Vegetable and Ornamental Crops, Council for Agricultural Research and Economics, Corso degli Inglesi 508, 18038 Sanremo, Italy; annalisa.giovannini@crea.gov.it (A.G.); andrea.copetta@crea.gov.it (A.C.)

* Correspondence: miriam.bazzicalupo@gmail.com (M.B.); jacopo.calevo@unito.it (J.C.)



Citation: Bazzicalupo, M.; Calevo, J.; Adamo, M.; Giovannini, A.; Copetta, A.; Cornara, L. Seed Micromorphology, *In Vitro* Germination, and Early-Stage Seedling Morphological Traits of *Cattleya purpurata* (Lindl. & Paxton) Van den Berg. *Horticulturae* **2021**, *7*, 480. <https://doi.org/10.3390/horticulturae7110480>

Academic Editor: Sergio Ruffo Roberto

Received: 11 October 2021

Accepted: 8 November 2021

Published: 10 November 2021

Publisher's Note: MDPI stays neutral with regard to jurisdictional claims in published maps and institutional affiliations.



Copyright: © 2021 by the authors. Licensee MDPI, Basel, Switzerland. This article is an open access article distributed under the terms and conditions of the Creative Commons Attribution (CC BY) license (<https://creativecommons.org/licenses/by/4.0/>).

Abstract: In the context of a symbiotic plant-fungus interaction study concerning *Cattleya purpurata*, we focused on some aspects of seed morphology and biology, and the early stages of seedling development. Seed morphology was characterized using light and scanning electron microscopy. *In vitro* seed germination capability was evaluated, comparing symbiotic and asymbiotic methods. The morphology of the seeds was overall comparable to that of other congeneric species, showing classical adaptations related to the aerodynamic properties and to the wettability of seeds, but calcium oxalate druses were identified inside the suspensor cells. Asymbiotic seed germination was successful in all tested media (17.1–46.5%) but was higher on 1/2 Murashige & Skoog. During symbiotic interaction with the fungal strain MUT4178 (*Tulasnella calospora*), germination rate was significantly lower than that obtained with the best three asymbiotic media, suggesting a low fungal compatibility. Seedling morphology was in line with other taxa from the same genus, showing typical characteristics of epiphytic species. Our observations, in particular, highlighted the presence of stomata with C-shaped guard cells in the leaves, rarely found in *Cattleyas* (where usually they are reniform), and confirm the presence of tilosomes in the roots. Idioblasts containing raphides were observed in both roots and leaves.

Keywords: crystals; microscopy; mycorrhizal fungi; orchids; suspensor

1. Introduction

Orchidaceae, with about 28,000 species and new ones being discovered every year, is one of the largest families of flowering plants [1]. The great majority of species is native to tropical or sub-tropical areas, but the family can be considered cosmopolitan, being spread over the five continents, with a distribution range that extends from the Arctic Circle to sub-Antarctic islands [2]. Orchids have interesting and often strict interactions with specialized pollinators and mycorrhizal fungi [3–5], and are at risk of extinction by intrinsic and extrinsic factors linked with habitat degradation [6], including weed invasion, grazing, altered hydrology, and altered fire regimes.

Among the Epidendroideae subfamily, the subtribe Laeliinae is strictly neotropical and comprises about 50 genera with about 1500 species [7,8]; it is one of the largest subtribes in the family after Pleurothallidinae and Oncidiinae [9]. Due to its morphological variability and taxonomic divergence [9], Laeliinae has been the subject of great taxonomic reviews

over the last few decades; in this subtribe, Dressler [7] included the genera *Cattleya* Lindl., *Laelia* Lindl., *Schomburgkia* Lindl., and *Sophronitis* Lindl. Van den Berg et al. [9,10], thanks to a phylogenetic analysis on ITS regions and considering the hybridization capability within Laeliinae, supported the inclusion of *Schomburgkia* and *Sophronitis* species in *Laelia* and *Cattleya*, respectively. For the above-mentioned reasons, Brazilian *Laelia* species, previously referred to as *Hadrolaelia* [11], have also been included in the genus *Cattleya* [12].

Cattleya purpurata (Lindl. & Paxton) Van den Berg (syn. *Laelia purpurata*) is a Brazilian orchid species that grows widely in the country and has been ranked as endangered (EN) by IUCN (International Union for Conservation of Nature) in the State of Rio Grande do Sul [13], due to its over-collection for commercial purpose [14]. The species has been the focus of many studies due to its high economical value; it is considered one of the flag flowers of Brazil and nowadays it is in collections all over the World, with several cultivars and varieties [15]. As recently reported by Caballero-Villalobos et al. [16], the species is nectarless and self-compatible, although it is pollinator-dependent. Some morphological investigations on the vegetative portions of this species have been carried out by Silva Júnior et al. [17] and Gallo et al. [18]. The former studied leaf characteristics and chlorophyll content of this species after the applications of different urea concentrations during *in vitro* experiments. Gallo et al. [18] performed an anatomical investigation on seed and protocorm from six species belonging to the genus *Cattleya*, *C. purpurata* included. Anatomical investigations provide important information to assess species identity, to better understand physiological processes, or to study phylogenetic relationships between taxa [19]. This information, which can be achieved considering both the vegetative and reproductive portions of a species, could also be used to improve knowledge and be applied in micropropagation techniques and conservation programs [18].

New propagation techniques have been proposed over the last decades to optimize asymbiotic and symbiotic seed germination, and to promote seedling acclimatization [15,20,21]. However, contrary to what is known about terrestrial species [22–24], few details are available concerning mycorrhizal associations in tropical orchids, especially in Laeliinae occurring in different environments (i.e., [25,26]).

In this work, which has been carried out in the framework of a plant-fungus interaction study [27], our aim was to obtain more morphological information regarding *C. purpurata* seed traits and test seed germination via both asymbiotic and symbiotic techniques, in the latter case using a fungal strain of the well-known orchid mycorrhizal (OM) fungus *Tulasnella calospora*. Seedlings grown on different media and growth conditions were then characterized from an anatomical and micro-morphological point of view in order to collect further data concerning this stage of development and to improve propagation techniques to be used in scientific and conservation programs.

2. Materials and Methods

2.1. Flower Hand Pollination and Seed Collection

Capsules were obtained by hand pollinated plants of *Cattleya purpurata* cultivated by the Azienda Agricola Nardotto e Capello in Camporosso (Imperia, Italy), 43° 48' 18" 00 N, 07° 37' 43" 32 E. At the time of capsule maturation, indicated by a yellowish color, three capsules were collected, and seeds were stored at 4 °C in a paper envelop until use [28].

2.2. Seed Sowing

After a sterilization in 1% NaClO solution, seeds were rinsed three times in sterile dH₂O for 5 min and then sowed on six different asymbiotic seed germination media: 1/2 strength of Murashige and Skoog [29], including vitamins (Duchefa) enriched with 50 mL/L of coconut water; Knudson C [30] orchid medium (Duchefa); Malmgren Modified medium [31]; M551 (Phytotechnology) enriched with 1mg/L BAP, which are commonly used for the propagation of epiphytic and terrestrial orchids [32]; and CG (CG0) and CG enriched with 50 mL/L (CG50) and 100 mL/L (CG100) almond milk, a new medium that showed to improve *in vitro* seedling development in both epiphytic and terrestrial

orchids [32]. All the media were supplemented with 2 g/L of activated charcoal and a total concentration of 10 g/L of sucrose; pH was adjusted to 5.8. Seeds were also sowed on an oat agar medium (OA), as described by Ercole et al. [33], with a mycorrhizal fungal strain of *Tulasnella calospora*, isolated at the University of Turin from *Serapias vomeracea* [34] and deposited in the mycological collection of the University of Turin (Mycotheca Universitatis Taurinensis, accession number MUT4178). Eight replicates for each medium were periodically checked under light microscope to assess germination percentage. The final germination percentage, recorded 70 days after seed sowing, was evaluated as the overall mean of single observations \pm SE. Seedlings were then moved to jars with the same media for three months before recording morphological data.

2.3. Microscopy

2.3.1. Plant Material

Nine months after sowing (after transferring seedlings on fresh media every three months), fully developed roots and leaves from each medium were sampled. Roots and leaves were cut about 1 cm from the apex and about half of their length, respectively. Plant material was prepared to perform micro-morphological investigations according to the following methods.

2.3.2. Light Microscopy

Light microscopy (LM) analysis was carried out on seeds, seedling leaves, and roots. Seeds were directly mounted onto a microscope slide after being rinsed in 5% NaClO solution for 1 h, and were then observed with a Leica DM 2000 transmission-light microscope coupled with a computer-driven DFC 320 camera (Leica Microsystems). Seed and embryo length, length/width (L/W) ratio, number of cells along the entire seed longitudinal axis, and length and number of cells of the suspensor were recorded for 100 seeds. Seed descriptive terminology has been used according to Barthlott et al. [35].

Transversal hand-sections of fresh leaves and roots obtained by a razor blade were stained with both TBO (Toluidine Blue O), to discriminate cell wall structures, and acid Phloroglucinol, to highlight xylem and lignified structures in general. The seeds and transversal sections of leaf and roots were also examined under a polarizing filter. In addition, to localize suberin and lignin, transversal sections of roots were stained with Fluorol Yellow 088 and observed under UV light.

2.3.3. Scanning Electron Microscopy

Seeds were incubated overnight in 100% ethanol, placed on aluminum stubs covered with double-sided carbon tape, and dried at room temperature, as performed by Calevo et al. [36]. Stubs were then sputter-coated with 10 nm gold particles and directly observed with a Vega3 Tescan LMU Scanning Electron Microscope (SEM) (Tescan USA Inc., Cranberry Twp, PA, USA) at an accelerating voltage of 20 kV, coupled to an X-ray Energy Dispersive System (EDS) Apollo XSD (Tescan USA Inc., Warrendale, PA, USA). A detailed assessment of seed ornamentation was carried out, considering the ornamentation of the periclinal walls and the type of anticlinal walls [37].

For SEM analysis of leaves and roots from in vitro grown seedlings, transversal sections of fresh material were fixed in FineFIX working solution (Milestone s.r.l., Bergamo, Italy) with 70% ethanol, and left overnight at 4 °C [38]. Sections were then dehydrated for 1 h through graded ethanol series from 70% to 100% at 60 min intervals, and finally dried using a Critical Point Dryer Processor (K850CPD 2M Strumenti S.r.l., Roma, Italy). Specimens were then mounted on stubs, as previously performed on seeds, to carry out micromorphological analyses.

2.4. Data Analysis

Germination data were statistically analyzed by ANOVA followed by Fisher's probable least-squares difference test, with a cut-off significance at $p \leq 0.001$.

Embryo and seed volumes were calculated following the equations reported in [37]:

$$\text{Embryo volume (EV)} = 4/3 \pi ab^2 \quad (1)$$

$$\text{Seed volume (SV)} = 2(\pi/3 r^2h) \quad (2)$$

where $a = 0.5 \times$ embryo length (or major axis); $b = 0.5 \times$ embryo width (or minor axis); $r = 0.5 \times$ seed width (or minor axis); and $h = 0.5 \times$ seed length (or major axis).

The morphological data of seeds were analyzed using the R environment [39]. Correlations between seed and embryo volumes were analyzed by means of the `cor.test` function, using the Spearman's rank correlation coefficient ρ [40,41]. Measures were expressed in $\mu\text{m} \pm \text{SD}$.

3. Results

3.1. Seed Germination

Cattleya purpurata seeds germinated on all the tested media. The best medium for asymbiotic germination was 1/2 MS, with a germination percentage of $46.5 \pm 6.4\%$. All the other asymbiotic media yielded lower germination percentages, ranging from $17.1 \pm 2.0\%$ (CG0) to $26.3 \pm 4.3\%$ (KC). The use of MUT4178 fungal strain of *T. calospora* resulted in a germination of $18.3 \pm 4.0\%$, statistically comparable with all the variants of CG medium (Table 1).

Table 1. Germination mean percentages (\pm Standard Error) ($n = 8$) recorded 70 days after seed sowing of *Cattleya purpurata*. Data were analyzed by ANOVA followed by Fisher's probable least-squares difference test with cut-off significance at $p \leq 0.001$. Percentages with the same letters are not significantly different from each other.

Medium	Germination %
1/2 MS	46.5 ± 6.4 a
KC	26.3 ± 4.3 b
M551	24.1 ± 2.6 b
CG0	17.1 ± 2.0 c
CG50	21.4 ± 2.9 bc
CG100	22.9 ± 5.3 bc
OA + MUT4178	18.3 ± 4.0 c

3.2. Morphology

3.2.1. Seed Morphology

Cattleya purpurata seeds, beige in color, are elongated (Figure 1a) and present a L/W ratio of 5.33 ± 0.62 . They showed an average seed length (excluding the suspensor) of $800.47 \pm 97.42 \mu\text{m}$, an average width of $154.75 \pm 22.37 \mu\text{m}$, an embryo length of $331.59 \pm 48.04 \mu\text{m}$, and an embryo width of $127.22 \pm 19.98 \mu\text{m}$ (Table 2). The comparison of seed and embryo volumes showed a significant positive relationship ($R = 0.74$, $p < 0.001$) (Supplementary Figure S1). The average suspensor length was $302.52 \pm 64.53 \mu\text{m}$; no significant relationship was found between suspensor length and both seed and embryo length and either between suspensor length and seed and embryo volumes.

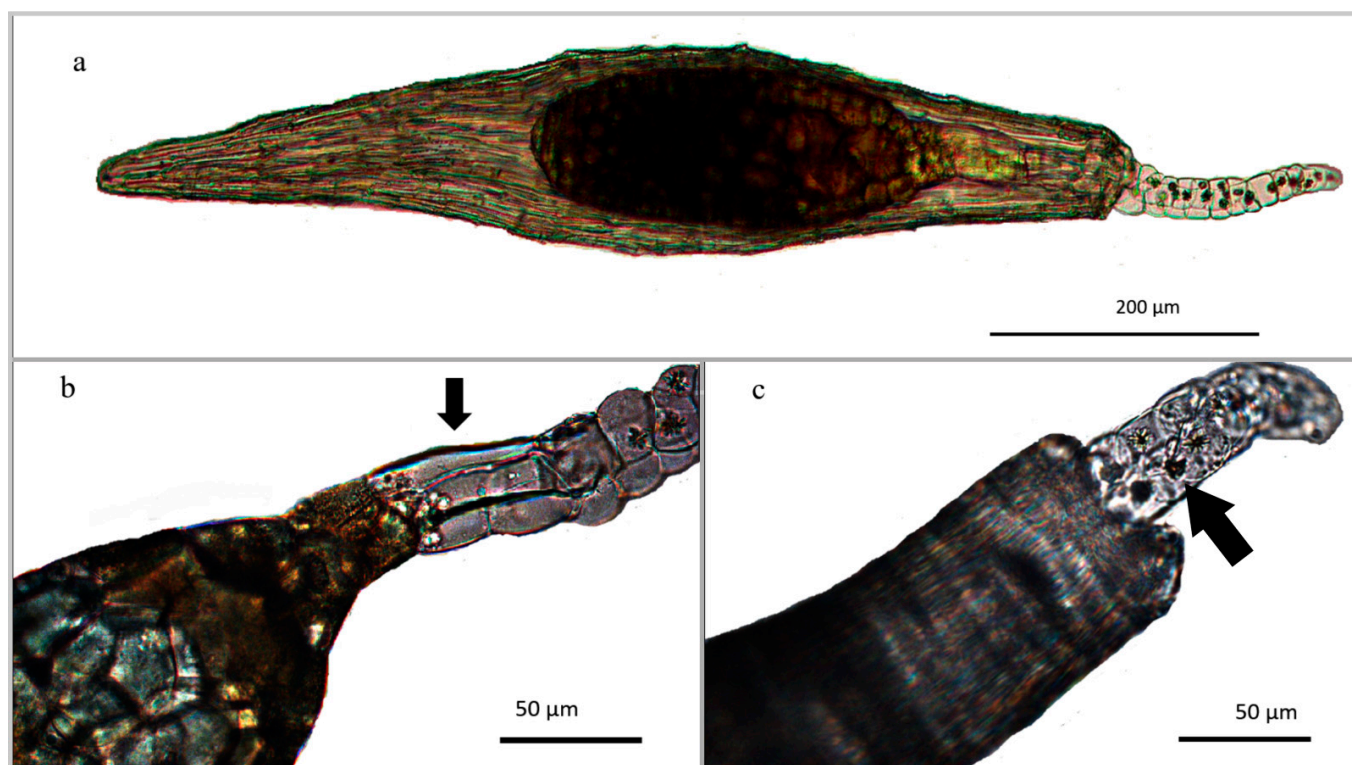


Figure 1. Light microscopy images of *Cattleya purpurata* seed. (a) LM overview of NaClO-treated seed, in which embryo is well distinguishable within the seed coat; (b) detail of the embryo body-suspensor connection (arrow) composed of 2–3 elongated cells. (c) untreated seed: View of the insertion of the suspensor inside the micropyle. Spherical druses are present in each cell of the suspensor (arrow).

Table 2. Means of seed morphological parameters ($n = 100$) and seed features of *Cattleya purpurata* (\pm Standard Deviation).

Seed Type	Elongated
Seed length (μm)	800.47 \pm 97.42
Seed width (μm)	154.74 \pm 22.37
Seed L/W ratio	5.33 \pm 0.62
Embryo length (μm)	331.59 \pm 48.04
Embryo width (μm)	127.22 \pm 19.97
Suspensor length (μm)	302.51 \pm 64.53
Seed testa cells	Without intercellular spaces
N ^o cells in longitudinal axis	>5
Suspensor layer	2–3 cell thick
Crystals	Calcium oxalate druses in the suspensor

Clarifying treatment with NaOCl allowed us to verify that seed coat was monolayered and that there were no intercellular gaps. Concerning *testa*, more than five cells were present along the seed longitudinal axis. These cells were elongated; their periclinal cell walls presented verrucosities and granular epicuticular coverings, while their anticlinal walls were occasionally elevated. As shown in Figure 2a,b, the seed coat enveloped the embryo, which showed a relatively long suspensor. Two-three elongated cells connected the embryo body with the portion of suspensor extending beyond the micropyle (Figure 1b, arrow).

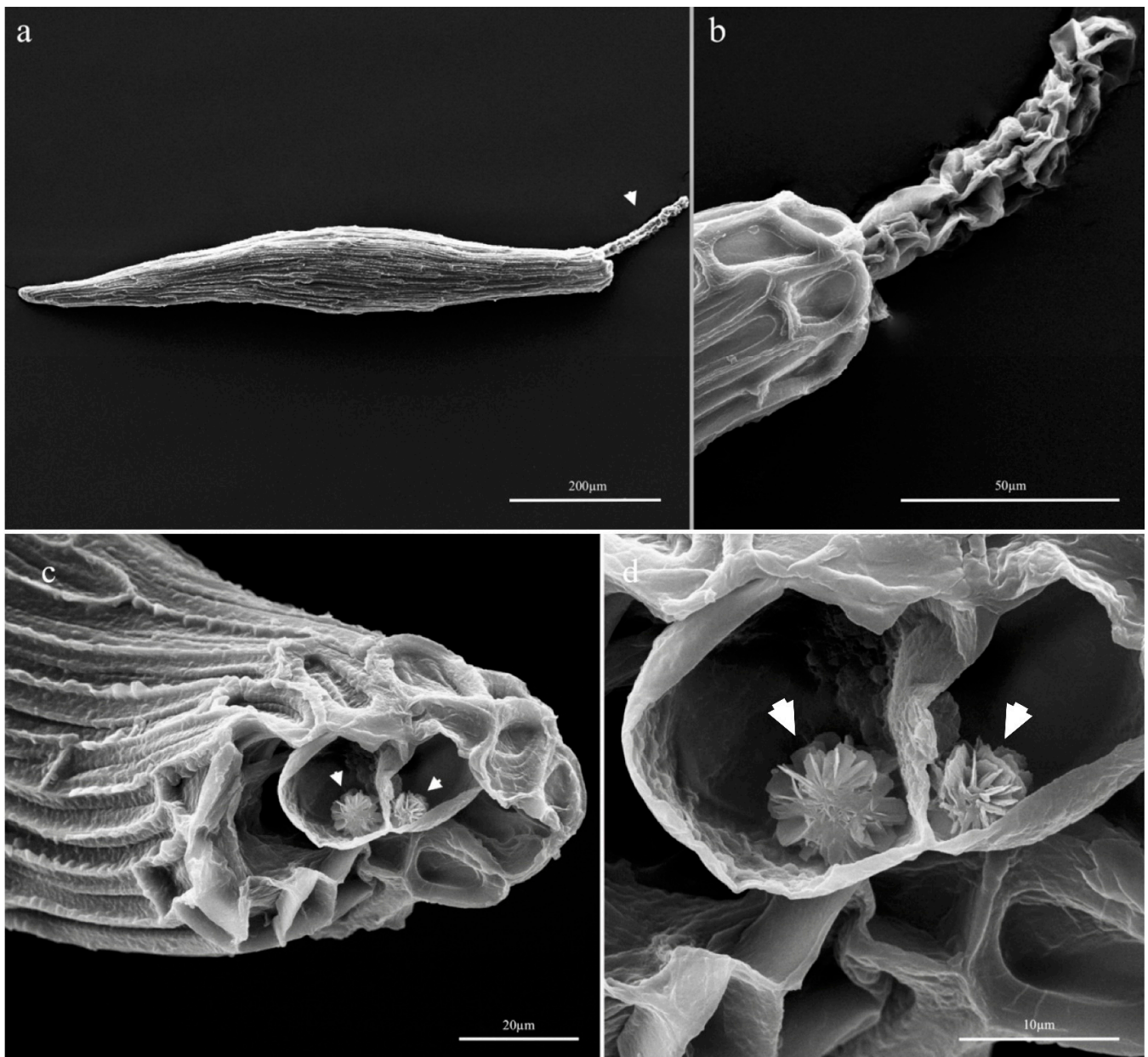


Figure 2. SEM micrograph of *Cattleya purpurata* seed. (a) overview of the seed showing the suspensor (arrow); (b) detailed view of the suspensor made of a 2–3 cells-thick layer; (c) cutaway of the suspensor highlighting the presence of druses (arrows) inside each cell. At higher magnification, the verrucose microrelief and the granular ornamentation of the seed coat cells are also visible; (d) particular of the druses (arrows).

The presence of spherical druses (6–8 nm in diameter) within the seed suspensor cells was recorded by both light (Figure 1a,c) and scanning electron microscopy (Figure 2c,d). SEM-EDS analysis of these crystals showed a high calcium peak, typical of the calcium oxalate spectrum (Supplementary Figure S2).

3.2.2. Root Sections

Microscopical analyses highlighted that the structure of roots sampled from *C. purpurata* seedlings grown on different substrates was qualitatively similar, except for the increased presence of hairs in individuals from CG50 and CG100 media (not shown). Velamen was two to four cells wide (Figure 3a); these cells appeared large, polygonal shaped, and radially elongated, and showed helical-banded wall thickenings (Figure 3b,g).

Exodermal cells were moderately large, polygonal-shaped, and \square -thickened (Figure 3b,d). Short thin-walled passage cells were scattered in the exoderm, near tilosomes of tufted type (Figure 3b, arrows) (according to Pridgeon et al. [42]). In the parenchymatous cortex, the presence of chloroplasts (Figure 3d) and raphides (Figure 3e) was recorded. Cortical cells varied in form and size: elements near to the endodermis were smaller than those of the middle layers (Figure 3a,d); some parenchymatous cells appeared more or less circular, while others were polygonal-shaped (Figure 3a,b,d). As confirmed by means of polarized light (not shown) and by Fluorol Yellow staining, some elements of the cortex presented suberized thickenings in cell walls (Figure 3c, arrows). Endodermis cells were square to tetragonal-shaped; passage cells were visible in correspondence of phloem clusters, while the other endodermis cells appeared O-thickened (Figure 3c). The pericycle presented thin-walled polygonal-shaped cells alternating with protoxylematic cell elements. This layer surrounded the central vascular cylinder characterized by a polyarch actinostele, which showed 10 xylem arches. In the root's central region, a parenchymal tissue composed by circular cells alternating with lignified elements was present (Figure 3c).

Roots of seedlings obtained from symbiotic cultures showed the presence of mycorrhizal hyphae on the external surface (Figure 3f). The beginning of hyphal coiling was also well visible on the wall thickening of the velamen cells (Figure 3g). Root features are summarized in Table 3.

Table 3. General seedling's root and leaf anatomical characters of *Cattleya purpurata* observed on all tested media (unless otherwise indicated).

Root	Characters
Hairs	From few to numerous if roots belonged to plants grown in CG50 and CG 100
Velamen cells	Moderately large, polygonal shaped, arranged in 2–3 layers. Helical thickenings in cell walls
Exodermis cells	Large, polygonal-shaped, arranged in monolayer. \square -thickened.
Cortex cells	Circular to polygonal shaped. Variable size. Presence of chloroplasts. Some elements show thickenings in the cell walls.
Central cylinder	Endodermis cell walls square to polygonal shaped, O-thickened; passage cells in correspondence of phloem; thin-walled pericycle cells alternating with protoxylematic elements.
Stele	Polyarch actynostele (10 arches)
Crystals	Raphides in the parenchymatic cortex cells
Other features	Tufted tilosomes near short thin-walled passage cells scattered in the exodermis
Leaf	
Cuticle	Granular ridged; 7–10 μm thick;
Stomata	Tetracytic apparatus. C-shaped guard cells. Present in the abaxial surface. Mean stomatal length: 23.5 ± 2.9 ; mean stomatal width: 26.5 ± 2.6 .
Epidermis	Cells rectangular/hexagonal shaped. Generally, one-layered (two-layered in the midvein zone)
Hypodermis	Present in correspondence of the midvein
Mesophyll	Dorsiventral in correspondence of the midvein, homogeneous towards the margins. Seven vascular bundles for each side of the midvein, arranged in a row. Transverse veins connecting principal vascular bundles. Abaxial row of schlerenchymatic fibers. Banded mesophyll cells.
Crystals	Idioblasts containing raphides

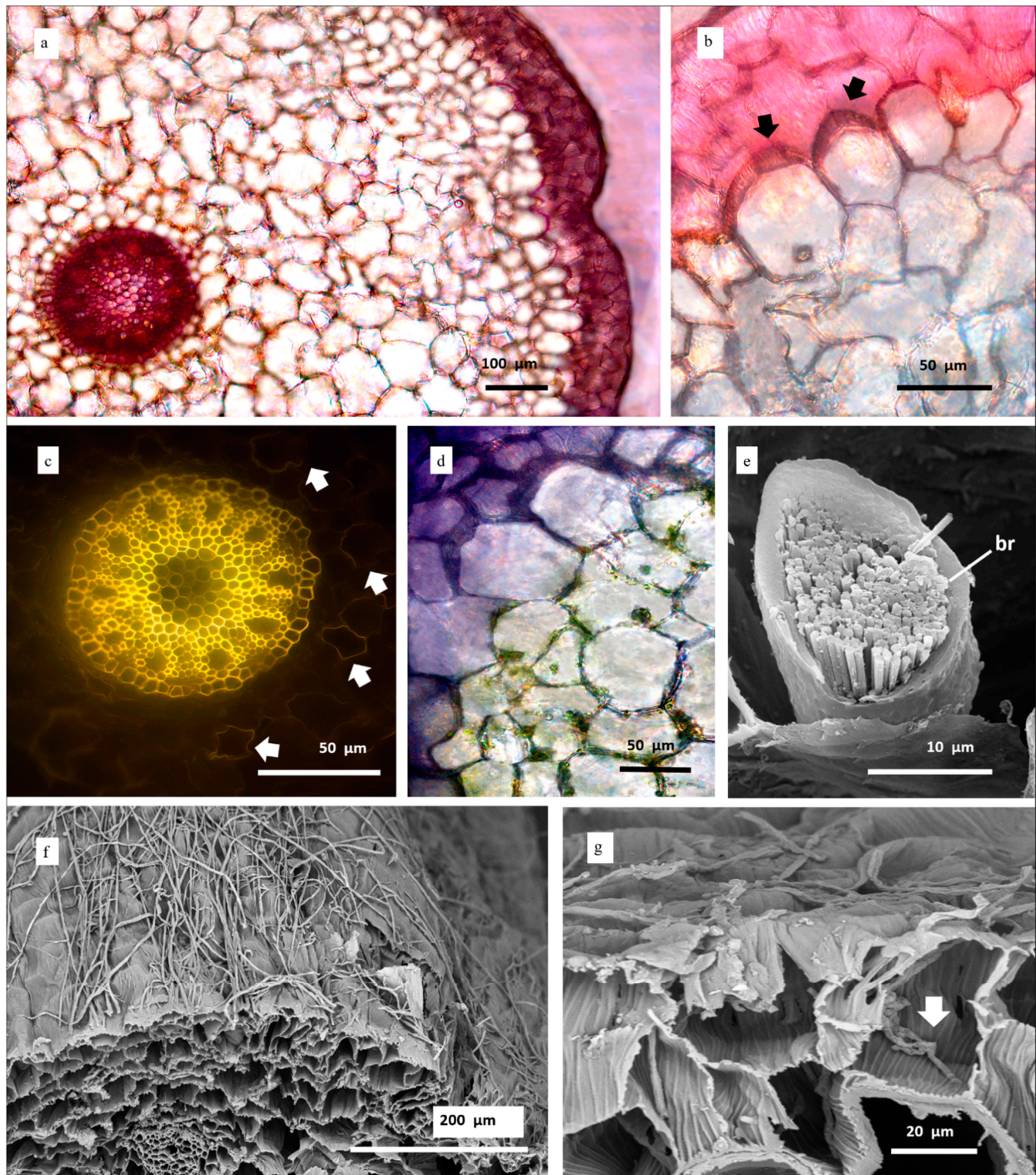


Figure 3. Root anatomy of *Cattleya purpurata* seedlings. Representative seedlings obtained on 1/2MS were selected for panels (a–e) and from OA medium for panels (f,g). (a) overview of the root’s transversal section stained with Phloroglucinol-HCl. Velamen is composed by a 2–3 cells wide layer; exoderm cells appear large, polygonal, and \cap -thickened; cortex cells from middle layers are larger than those near to the exoderm and to the endoderm. The vascular cylinder is composed by a polyarch actynostele; (b) tufted tilosomes (arrows) observed in the endovelamen-exoderm region; (c) Fluorol Yellow staining: detail of the central vascular cylinder characterized by a polyarch actinostele. The central parenchymatic tissue is composed by circular cells alternating with lignified elements. Cortex elements showing suberized cell walls are also visible (arrows); (d) chloroplasts within cortex cells; (e) SEM photograph of bundled raphides (br) within a cell of cortical parenchyma; (f) SEM image of mycorrhizal hyphae in the first stages of colonization of a root obtained from symbiotic culture; (g) the beginning of hyphal coiling inside a velamen cell (arrow). Banded wall thickenings of velamen cells are also distinguishable.

3.2.3. Leaf Surface and Transversal Sections

The media used for seed germination and seedling development did not lead to structural changes in leaves. Leaf surfaces were composed of mostly rectangular to hexagonal cells and showed a ridged, granular cuticle, $7.0 \pm 1.3 \mu\text{m}$ thick in the abaxial surface and $10.0 \pm 1.6 \mu\text{m}$ in the adaxial one (Figure 4a,b). Tetracytic stomata with C-shaped guard cells were present only in the lower epidermis; the stomatal aperture was parallel to the longitudinal axis of the leaf (Figure 4a). Mean stomatal length was $23.5 \pm 2.9 \mu\text{m}$, while mean stomatal width was $26.5 \pm 2.6 \mu\text{m}$. In transversal section, on both sides of the midvein, seven vascular bundles arranged in a row were visible (Figure 4c). The central midvein (Figure 4c,d), positioned near the lower surface, was surrounded by several hypodermal cell layers (not shown). In correspondence of the central midvein, the epidermis was bistratified. The leaf presented a dorsiventral mesophyll at the level of the central midvein and a homogeneous one towards the margins. Parenchyma cells gradually increased in diameter while approaching the central portion, where isodiametric and elongated thick-walled cells were present near the midvein, resembling a palisade parenchyma (Figure 4c). In many cases, we observed vessel elements developed transversely, which connected the small veins (Figure 4e). Vascular collateral bundles showed sclerenchyma caps at both xylem and phloem poles, but predominantly at the phloem one (Figure 4d,e). Little sclerenchyma fiber bundles were present as an abaxial row (not shown), while two clearly distinguishable bundles were positioned at each leaf margin: a little bundle in the margin tip and a larger one more internal (Figure 4c,f). Idioblasts containing raphides were interspersed in the mesophyll (Figure 4f, arrow). Leaf features are summarized in Table 3.

As highlighted by SEM analyses, some mesophyll cell walls were banded (Figure 4g).

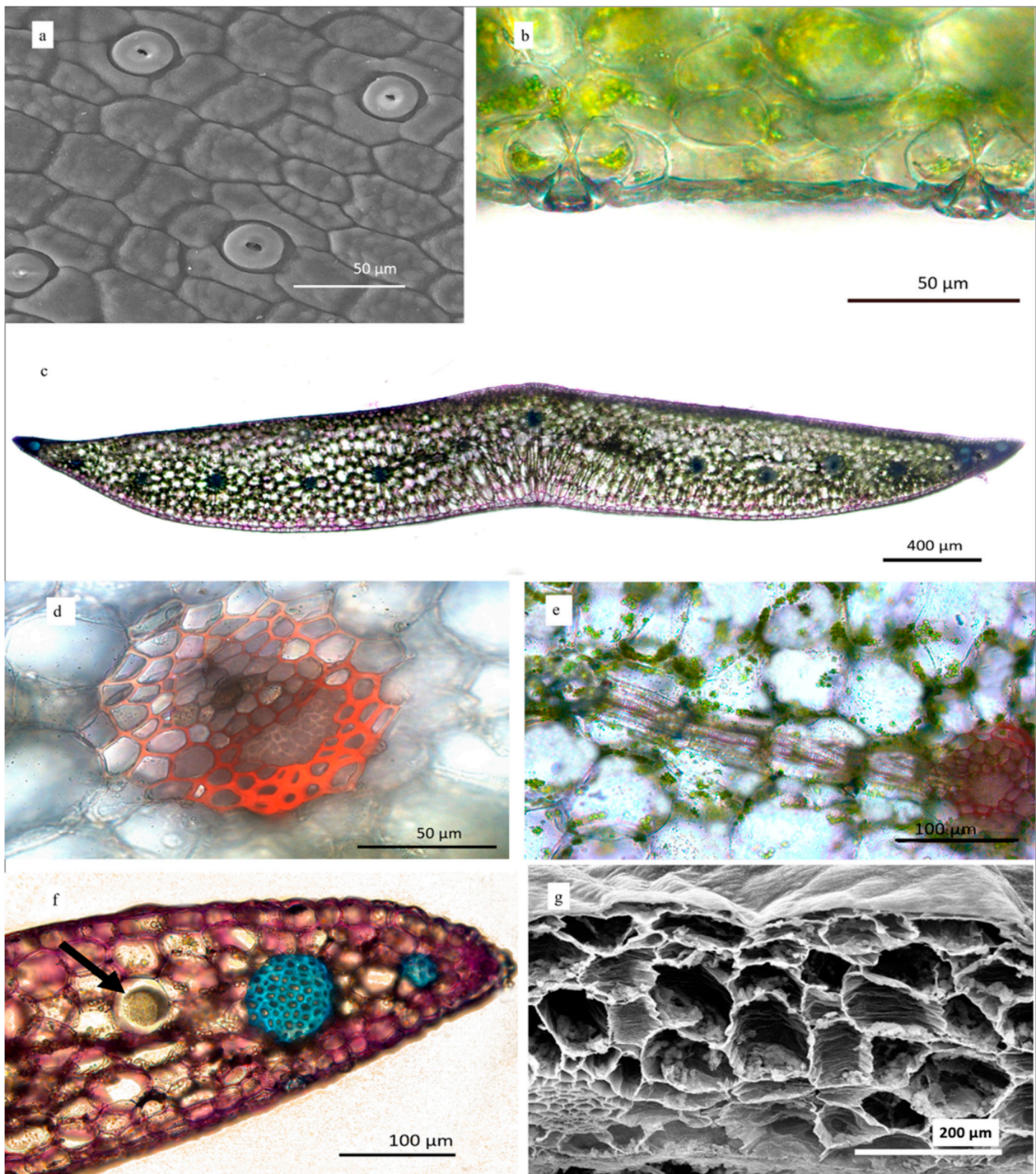


Figure 4. Leaf anatomy of *Cattleya purpurata* seedlings. Representative seedlings obtained on M551 medium were selected for images. (a) SEM picture of the lower surface of the leaf, revealing hexagonal cells covered by a thick granular cuticle and the tetracytic stomatal apparatus with C-shaped guard cells; (b) transversal section: detail of the leaf's abaxial portion, in which stomata are visible. Cuticle is 6–9 μm thick; (c) transversal section stained with TBO. Seven vascular bundles arranged in a row are visible. The central midvein is positioned near the lower surface. A dorsiventral mesophyll is present at the level of the central midvein, while a homogeneous one is distinguishable towards the margins. Two sclerenchymatic bundles are present at each leaf tip; (d) View of the central midvein stained with HCl-phloroglucinol; (e) transversely developed vessel elements, connecting with a vascular bundle red-stained with HCl-phloroglucinol; (f) transversal section of the leaf stained with TBO. The two sclerenchymatic bundles are visible near the leaf margin; (g) SEM picture of the mesophyll in cross section: banded thickenings are distinguishable in some cells.

4. Discussion

As observed by Gallo et al. [18] and confirmed by our analyses, the seed coat of the studied species consists of only one cell layer. As reminded by the latter authors, the reduced and membranous seed coat of Laeliinae seeds and the air space between the tegument and the embryo is an adaptation related to the aerodynamic properties and to the wettability of seeds [37,43]. While a significant correlation has been found between seed and embryo length, suspensor length was not correlated to seed or embryo size, indicating that suspensor dimension does not influence seed development in *C. purpurata*.

Although Gallo et al. [18] already described the long multicellular suspensor in *C. purpurata* and other specimens belonging to the Laeliinae subtribe, the presence of calcium oxalate druses for each cell of the structure had not yet been reported. To the best of our knowledge, this study is the first reporting the occurrence of druses in the suspensor, or more generally, in orchid seeds. In fact, such crystal conglomerates, according to Prychid and Rudall [44], are commonly found in various dicotyledons tissues but are more rarely observed in monocotyledons; concerning family Orchidaceae, druses have been recorded only in vegetative portions of Epidendreae and Dendrobieae [45,46], Arethusae [46], and in the >23% of the Oncidiinae [47].

Lee et al. [48], studying the suspensor of *Paphiopedilum delenatii*, observed that there was no cuticular material in the cell walls of the structure; considering the morphological traits of the transfer cell, they finally hypothesized that the suspensor was responsible for nutrient uptake for the embryo. Later, the role of embryo suspensor in nutrition has been confirmed [49,50]. In addition, Volk et al. [51] demonstrated that the deposition of druses in idioblasts is a dynamic process and, when Ca availability is reduced, cells could dissolve the crystals metabolizing CaOx to non-toxic compounds. According to these authors and considering our observations, it is possible that the suspensor possesses storage potential and, while providing a channel for nutrients conduction to embryo, could store the excess of calcium coming from the environment or could receive it as a byproduct of seed metabolism. Calcium oxalate, on the other hand, has many functional roles also for fungi, such as metal detoxification or increasing plant susceptibility to fungal infection, acting as an electron donor in lignocellulose degradation [52] and in the reduction of certain metals [53]. Oxalate, indeed, plays a unique role in lignocellulose degradation by basidiomycetes, acting as a low molecular mass agent initiating decay and as a potential electron donor for lignin-peroxidase catalyzed reduction [54–56]. This is particularly interesting because fungal colonization of orchid seeds by orchid mycorrhizal fungi (belonging to the Basidiomycota) occurs through the suspensor [57–60]. It is tempting to hypothesize that the druses have evolutionarily assumed the role of ready-to-use oxalate reserves available to the symbiont fungi to favor the degradation of the lignocellulose present in the seed coat [61] and their settlement as symbionts. It should be remembered that, in mycorrhizal fungi, the energy balance is very important [22] and even more so in orchid mycorrhizal fungi, where the debate in the scientific community is still ongoing [22,62,63]. Possibly supporting this hypothesis, Miura et al. [64] found that the presence of seed coat enhances seed germination with symbiotic fungi and protects the embryo against the attack of non-symbiotic fungi by restricting the invasion of their fungal hyphae. Indeed, the seed coat is a barrier against fungi that do not possess enzymes capable of degrading lignocellulose, making a sort of selection at the entrance.

However, as the druses deposition was recorded starting from the first two cells after the elongated pair and all along the suspensor (see Figure 3a,b), we cannot exclude that its detachment from the developing embryo in the early stages of germination might be a fast way to remove the excess of calcium oxalate. This hypothesis agrees to that discussed by Paiva [65], who concluded that the formation of CaOx crystals in portions that will be discarded allows the excretion of calcium, because plants lack excretory systems.

Germination was successful on all the media tested, but 1/2 MS was the best and is therefore suggested for *C. purpurata* propagation. Germination occurred also by using the fungal strain MUT4178 of *Tulasnella calospora* but with a lower percentage if compared to

the above-mentioned asymbiotic medium. Almeida et al. [26] indicated Tulasnellaceae (including *T. calospora*) as the main possible fungal symbionts for this orchid group; however, our results, which report the first attempt of symbiotic germination for *C. purpurata* (to the best of our knowledge) may indicate that the fungal strain used, isolated from an European terrestrial orchid, might not be the most appropriate or the dominant symbiont for this species, even if we demonstrated its colonization of roots (see also Adamo et al. [27]).

The subsequent development of seedlings grown *in vitro* allowed characterization of their morphology. According to the literature, this is the first study providing morphological information regarding *in vitro* seedlings of *C. purpurata*, because Gallo et al. [18] worked on the same species but in earlier stages of protocorm development, while Silva Júnior et al. [17] compared the anatomy of roots and leaves from plants treated with different urea concentrations.

We observed idioblasts containing raphides in both root and leaf tissues, adding information regarding their presence in the early development stages of seedlings. The occurrence, distribution, and morphology of idioblasts containing raphides have been reported by various authors who studied the vegetative tissues of most of the analyzed orchid subtribes [66] (and references therein). Stern and Carlsward [67] carried out a comparative study concerning vegetative portions of members from Laeliinae, and found that crystalliferous idioblasts, circular in transverse section and saccate in the longitudinal one, are present ubiquitously in the mesophyll of all the examined taxa. In general, the role of raphides for plant tissues also needs to be clarified. As recently revised by Paiva [65], various hypotheses about the functions of raphides in plant tissues have been indeed formulated; they could help in regulating calcium levels [51] or constitute a CO₂ source for photosynthesis in some species [68]. Tulyananda and Nilsen [69] stated that idioblasts spread in thin leaves of epiphytic species (in this case, *Rhododendron* sp.) act as buffering agents that significantly affect leaf-lamina water relations. As previously proposed by several authors and recently revised by Konno et al. [70], raphides could play a defensive role against herbivory.

Some of the anatomical characters observed in the roots and leaves of the studied species are typical to those of epiphytic orchid habit.

Root presented a 2–3 layered velamen, showing helical cell wall thickenings. Such a restricted number of velamen layers is characteristic of species belonging to relatively humid habitats [71]. Velamen avoids the loss of moisture from roots, speeds up water absorption, and provides protection against mechanical stresses and ultraviolet radiations [72,73]. On the other hand, helical thickenings in the velamen cells have the function to improve the stability and efficiency of this tissue for water absorption by the root and its retention in dry conditions in epiphytic orchids [74]. Passage cells constitute a channel for the selective transit of nutrients and water, and for the entrance of mycorrhizal fungi [71,75,76]. Tilosomes, branched lignified wall ingrowths on the internal periclinal wall of the endovelamen cells, are typically positioned near passage cells [77,78]. These structures, according to Kedrovski and Sajo [78], increase symplastic connections and improve water and solutes transport between external and internal environments in young tissues, while they steer solutes to passage cells in mature tissues. Stern and Carlsward [67] stated that there are no tilosomes in *Cattleya* but annotated their occurrence in other species that have been moved in this genus in times after their work, i.e., *Sophranitis sincorana* (now *C. sincorana*) and *Laelia anceps* (now *C. anceps*). Our observation confirms the fact that tilosomes are also present in *Cattleya* genus.

The monolayered exodermis with large elements with \cap -thickened cell walls is also typical of epiphytic orchids. This structure prevents transpiration and water loss from the cortex [71].

Taken together, the characteristics of exodermis, the number of velamen layers, the occurrence and orientation of thickenings in velamen cell walls, and the presence of tilosomes possess taxonomical value according to Porembsky and Barthlott [77]. To classify orchid roots, the latter authors indeed considered combinations of the aforementioned

characters, proposing 12 different syndromes; the complex of features showed by our study species resembles that of *Vanda*-type.

A high presence of chloroplasts was recorded in the cortex. This aspect is well known for Laeliinae [67] and in general for epiphytic orchids; many species have evolved photosynthetic roots to increase photosynthetic areas and consequently carbon gain [72,79,80].

The variable shape and the presence of thickened birefringent cell walls of cortex elements agree with what has been reported for other Laeliinae members by Stern and Carlswald [67]. Additionally, both endodermis and pericycle cells show characteristics already described by the latter authors (similar in dimension and O-thickened); however, contrary to what has been observed in general for Laeliinae, we recognized O-thickenings in correspondence of xylem rays instead of phloem ones, and protoxylematic elements in the pericycle. Lignin deposition in other elements of the central cylinder and endodermal cell wall thickenings may play similar functions to those of velamen and exodermis (prevention of water loss) and constitute another adaptative trait to tropical habitat conditions [71].

The number of xylem arches (10) falls in the range of 7–24, reported for this group of orchids [67]. Gallo et al. [18] recorded a triarch-tetrarch actynostele in developing protocorms, but it should be remembered that the organization of the vascular system undergoes changes during plant development [81].

Additionally, leaf characteristics are in line with the ecological adaptations of *C. purpurata* to a tropical environment. The roughness and thickness of *C. purpurata* leaf cuticles are consistent with characters and data previously annotated for Laeliinae [67]. The cuticle, relatively thick if compared to other orchid species [82], plays an ecological role in transpiration reduction and in drought resistance [83–85]. Similar considerations could be drawn for stomata dimensions, as small stomata are known to be quicker to close and then are more tolerant to dry conditions [84].

The stomatal apparatus is tetracytic, as noted in most Laeliinae; however, while a reniform shape was described for all the other taxa [66,67], the C-shaped guard cells that we observed were previously reported only for *Cattleya sincorana* (syn. *Sophronitis sincorana*). This latter record can be useful to corroborate taxonomical information regarding the studied species.

The data regarding the discontinuous hypodermis, the homogeneous mesophyll, and the dorsiventral one in correspondence of the central rib, together with the characteristics of vascular system, agree to what is generally known for Laeliinae [67]. On the other hand, the presence of transversally developed elements, which constitute anastomoses between veins in the mesophyll, was less frequently annotated in the subtribe. It has been proposed that they provide mechanical stability and discourage herbivory [86]. The occurrence of transverse veins in the mesophyll of *C. purpurata* is in line with previous findings for the genus *Cattleya* [87].

5. Conclusions

In conclusion, we compared germination on different media and, for the first time, attempted symbiotic germination for *Cattleya purpurata*, demonstrating the potential use of Tulasnellaceae, which otherwise need to be refined, looking for the best symbiotic fungal partner because germination percentage was lower than that obtained on some asymbiotic media. Furthermore, we characterized its seed and seedling morphology, providing new insights into the knowledge of this endangered species. Seedling morphology was comparable with other congeneric species, showing typical characteristics of epiphytic orchids such as root velamen with 2–3 cells layers. We confirmed the presence of tilosomes in roots in this orchid genus and observed stomata with C-shaped guard cells in leaves, which are unusually found in *Cattleya* species. Interestingly, we pointed out the presence of calcium oxalate crystals, both in idioblasts as raphides (in roots and leaves) and in the seed suspensor as druzes. It would be intriguing, in the future, to see if other orchid species actually accumulate these crystals in the suspensor and if they have a nutritional/functional role in the orchid symbiosis.

Supplementary Materials: The following are available online at <https://www.mdpi.com/article/10.3390/horticulturae7110480/s1>, Figure S1: Correlation between the volume of the embryo and the seed analyzed by means of the `cor.test()` function using the Spearman's rank correlation coefficient ρ , Figure S2: Main elements present in crystals determined by SEM-EDS spectrum. The analysis showed a chemical composition typically obtained for calcium oxalate, with carbon (C), oxygen (O) and calcium (Ca) peaks.

Author Contributions: Conceptualization, J.C. and M.B.; methodology, J.C., M.B., A.C. and L.C.; software, J.C., M.B. and M.A.; validation, J.C., M.B. and L.C.; formal analysis, J.C. and M.B.; investigation, J.C. and M.B.; resources, J.C., L.C. and A.G.; data curation, J.C. and M.B.; writing—original draft preparation, J.C. and M.B.; writing—review and editing, M.B., J.C., M.A., A.G., A.C. and L.C.; visualization, J.C., M.B., M.A., A.C. and L.C.; supervision, L.C. All authors have read and agreed to the published version of the manuscript.

Funding: This research received no external funding.

Institutional Review Board Statement: Not applicable.

Informed Consent Statement: Not applicable.

Data Availability Statement: Not applicable.

Acknowledgments: The experimental work for this study has been performed within the framework of the doctoral research projects of J. Calevo (PhD School in Biology and Applied Biotechnologies, University of Turin) and M. Bazzicalupo (PhD School in Science and Technology for the Environment and Territory, University of Genoa), both funded by the Ministry of Education and Research (MIUR). M. Adamo was supported by a grant from CMIRA (Coopération et Mobilité Internationales Rhône-Alpes) program of region Rhône-Alpes, France. We thank Laura Negretti for SEM images.

Conflicts of Interest: The authors declare no conflict of interest.

References

1. Christenhusz, M.J.M.; Byng, J.W. The number of known plants species in the world and its annual increase. *Phytotaxa* **2016**, *261*, 201–217. [[CrossRef](#)]
2. Nicholson, C.C.; Bales, J.W.; Palmer-Fortune, J.E.; Nicholson, R.G. Darwin's bee-trap: The kinetics of *Catasetum*, a new world orchid. *Plant Signal. Behav.* **2008**, *3*, 19–23. [[CrossRef](#)] [[PubMed](#)]
3. Rasmussen, H.N. Cell differentiation and mycorrhizal infection in *Dactylorhiza majalis* (Rchb. F.) Hunt & Summerh. (Orchidaceae) during germination in vitro. *New Phytol.* **1990**, *116*, 137–147.
4. Leake, J.R. The biology of myco-heterotrophic ('saprotrophic') plants. *New Phytol.* **1994**, *127*, 171–216. [[CrossRef](#)] [[PubMed](#)]
5. Girlanda, M.; Selosse, M.A.; Cafasso, D.; Brilli, F.; Delfino, S.; Fabbian, R.; Ghignone, S.; Pinelli, P.; Segreto, R.; Loreto, F.; et al. Inefficient photosynthesis in the Mediterranean orchid *Limodorum abortivum* is mirrored by specific association to ectomycorrhizal Russulaceae. *Mol. Ecol.* **2006**, *15*, 491–504. [[CrossRef](#)]
6. Swarts, N.D.; Dixon, K.W. Terrestrial orchid conservation in the age of extinction. *Ann. Bot.* **2009**, *104*, 543–556. [[CrossRef](#)]
7. Dressler, R.L. *The Orchids. Natural History and Classification*, 2nd ed.; Harvard University Press: Cambridge, UK, 1981; p. 334.
8. Dressler, R.L. *Phylogeny and Classification of the Orchid Family*, 1st ed.; Dioscorides Press: Portland, OR, USA, 1993; p. 330.
9. Van den Berg, C.; Higgins, W.E.; Dressler, R.L.; Whitten, W.M.; Soto-Arenas, M.A.; Chase, M.W. A phylogenetic study of Laeliinae (Orchidaceae) based on combined nuclear and plastid DNA sequences. *Ann. Bot.* **2009**, *104*, 417–430. [[CrossRef](#)] [[PubMed](#)]
10. Van den Berg, C.; Goldman, D.H.; Freudenstein, J.V.; Pridgeon, A.M.; Cameron, K.M.; Chase, M.W. An overview of the phylogenetic relationships within Epidendroideae inferred from multiple DNA regions and recircumscription of Epidendreae and Arethuseae (Orchidaceae). *Am. J. Bot.* **2005**, *92*, 613–624. [[CrossRef](#)]
11. Chiron, G.R.; Castro Neto, V.P. Révision des espèces brésiliennes du genre *Laelia* Lindley. *Richardiana* **2002**, *2*, 4–28.
12. Van den Berg, C. New combinations in the genus *Cattleya* Lindl. *Neodiversity* **2008**, *3*, 3–12. [[CrossRef](#)]
13. Rio Grande do Sul. *Decreto 52.109, de 2 de Dezembro de 2014. Declara as Espécies da Flora Nativa Ameaçadas de Extinção do Estado do Rio Grande do Sul*; Diário Oficial do Estado do Rio Grande do Sul: Porto Alegre, Brazil, 2014; Volume 72, pp. 2–11.
14. Hosomi, S.T.; Custódio, C.C.; Seaton, P.T.; Marks, T.R.; Barbosa Machado-Neto, N. Improved assessment of viability and germination of *Cattleya* (Orchidaceae) seeds following storage. *Vitr. Cell Dev. Biol.-Plant* **2012**, *48*, 127–136. [[CrossRef](#)]
15. Seidel Junior, D.; Venturieri, G.A. Ex vitro acclimatization of *Cattleya forbesii* and *Laelia purpurata* seedlings in a selection of substrates. *Acta Sci. Agron.* **2011**, *33*, 97–103.
16. Caballero-Villalobos, L.; Silva-Arias, G.A.; Buzatto, C.R.; Nervo, M.H.; Singer, R.B. Generalized food-deceptive pollination in four *Cattleya* (Orchidaceae: Laeliinae) species from Southern Brazil. *Flora* **2017**, *234*, 195–206. [[CrossRef](#)]
17. Silva Júnior, J.M.; da Rodrigues, M.; de Castro, E.M.; Bertolucci, S.K.V.; Pasqual, M. Changes in anatomy and chlorophyll synthesis in orchids propagated *in vitro* in the presence of urea. *Acta Sci. Agron.* **2013**, *35*, 65–72. [[CrossRef](#)]

18. Gallo, F.R.; Souza, L.A.; Milaneze-Gutierrez, M.A.; Almeida, O.J.G. Seed structure and in vitro seedling development of certain Laeliinae species (Orchidaceae). *Rev. Mex. Biodivers.* **2016**, *87*, 68–73. [[CrossRef](#)]
19. Kowsalya, A.; Rojamalla, K.; Thangavelu, M. Comparative vegetative anatomy of South Indian Vandas (Orchidaceae). *Flora* **2017**, *235*, 59–75. [[CrossRef](#)]
20. Stancato, G.C.; Chagas, E.P.; Mazzafera, P. Development and germination of seeds of *Laelia purpurata* (Orchidaceae). *Lindleyana* **1998**, *13*, 97–100.
21. Gonçalves, L.D.M.; Prizão, E.C.; Milaneze Gutierrez, M.A.; Mangolin, C.A.; da Silva Machado, M.d.F.P. Use of complex supplements and light-differential effects for micropropagation of *Hadrolaelia purpurata* (= *Laelia purpurata*) and *Encyclia randii* orchids. *Acta Sci. Agron.* **2012**, *34*, 459–463. [[CrossRef](#)]
22. Smith, S.E.; Read, D.J. *Mycorrhizal Symbiosis*, 2nd ed.; Academic Press: Cambridge, UK, 2008.
23. Dearnaley, J.D.W.; Martos, F.; Selosse, M.A. Orchid mycorrhizas: Molecular ecology, physiology, evolution, and conservation aspects. In *Fungal Associations*, 2nd ed.; Hock, B., Ed.; Springer: Berlin, Germany, 2012; pp. 207–230.
24. Rasmussen, H.N.; Rasmussen, F.N. Seedling mycorrhiza: A discussion of origin and evolution in Orchidaceae. *Bot. J. Linn. Soc.* **2014**, *175*, 313–327. [[CrossRef](#)]
25. Withner, C.L. *The Cattleyas and Their Relatives. Vol. VI. The South American Encyclia Species*; Timber Press: Portland, OR, USA, 2000.
26. Almeida, P.R.M.; Van den Berg, C.; Goes-Neto, A. Morphological and molecular characterization of species of *Tulasnella* (Homobasidiomycetes) associated with neotropical plants of Laeliinae (Orchidaceae) occurring in Brazil. *Lankasteriana* **2007**, *7*, 22–27.
27. Adamo, M.; Chialva, M.; Calevo, J.; De Rose, S.; Girlanda, M.; Perotto, S.; Balestrini, R. The Dark Side of orchid symbiosis: Can *Tulasnella calospora* decompose host tissues? *Int. J. Mol. Sci.* **2020**, *21*, 3139. [[CrossRef](#)] [[PubMed](#)]
28. Calevo, J.; Giovannini, A.; Cornara, L.; Peccenini, S. Asymbiotic seed germination of hand-pollinated terrestrial orchids. *Acta Hort.* **2017**, *1155*, 415–418. [[CrossRef](#)]
29. Murashige, T.; Skoog, F. A revised medium for rapid growth and bioassays with tobacco tissue cultures. *Physiol. Plant.* **1962**, *15*, 473–497. [[CrossRef](#)]
30. Morel, G. Clonal propagation of orchids by meristem culture. *Cymbidium Soc. News* **1965**, *20*, 3–11.
31. Malmgren, S. Orchid propagation: Theory and practice. In *North American Native Terrestrial Orchids: Propagation and Production, Proceedings of the North American Native Terrestrial Orchid Conference, Germantown, MD, USA, 16–17 March 1996*; Allen, C., Ed.; pp. 63–71.
32. Calevo, J.; Copetta, A.; Marchioni, I.; Bazzicalupo, M.; Pianta, M.; Shirmohammadi, N.; Cornara, L.; Giovannini, A. The use of a new culture medium and organic supplement to improve in vitro early stage development of five orchid species. *Plant Biosyst.* **2020**. [[CrossRef](#)]
33. Ercole, E.; Rodda, M.; Girlanda, M.; Perotto, S. Establishment of a symbiotic in vitro system between a green meadow orchid and a *Rhizoctonia*-like fungus. *Bio-Protocol* **2015**, *5*, e1482. [[CrossRef](#)]
34. Girlanda, M.; Segreto, R.; Cafasso, D.; Liebel, H.T.; Rodda, M.; Ercole, E.; Cozzolino, S.; Gebauer, G.; Perotto, S. Photosynthetic mediterranean meadow orchids feature partial mycoheterotrophy and specific mycorrhizal associations. *Am. J. Bot.* **2011**, *98*, 1148–1163. [[CrossRef](#)]
35. Barthlott, W.; Große-Veldmann, B.; Korotkova, N. *Orchid Seed Diversity: A Scanning Electron Microscopy Survey*, 1st ed.; Englera. Botanischer Garten und Botanisches Museum: Berlin, Germany, 2014.
36. Calevo, J.; Giovannini, A.; Cornara, L.; Peccenini, S.; Monroy, F. *Orchis patens* Desf.: Seed morphology of an endangered Mediterranean orchid. *Plant Biosyst.* **2017**, *151*, 761–765. [[CrossRef](#)]
37. Arditti, J.; Ghani, A.K.A. Numerical and physical properties of orchid seeds and their biological implications. *New Phytol.* **2000**, *145*, 367–421. [[CrossRef](#)]
38. Chieco, C.; Rotondi, A.; Morrone, L.; Rapparini, F.; Baraldi, R. An ethanol-based fixation method for anatomical and micro-morphological characterization of leaves of various tree species. *Biotech. Histochem.* **2013**, *88*, 109–119. [[CrossRef](#)]
39. R Core Team. *R: A Language and Environment for Statistical Computing*; R Foundation for Statistical Computing: Vienna, Austria, 2020. Available online: <http://www.R-project.org/> (accessed on 16 January 2021).
40. Best, D.J.; Roberts, D.E. Algorithm AS 89: The upper tail probabilities of Spearman's rho. *J. R. Stat. Soc.* **1975**, *24*, 377–379. [[CrossRef](#)]
41. Hollander, M.; Wolfe, D.A. *Nonparametric Statistical Methods*; John Wiley & Sons: New York, NY, USA, 1973; pp. 185–194.
42. Pridgeon, A.M.; Stern, W.L.; Benzing, D.H. Tilosomes in roots of Orchidaceae: Morphology and systematic occurrence. *Am. J. Bot.* **1983**, *70*, 1365–1377. [[CrossRef](#)]
43. Barthlott, W. Morphologie der Samen von orchideen in Hinblick auf taxonomische und funktionelle Aspekte. In *Proceedings of the 8th World Orchid Conference, Frankfurt, Germany, 10–17 April 1975*; Senghas, K., Ed.; German Orchid Society Inc.: Frankfurt, Germany, 1976; pp. 444–455.
44. Prychid, C.J.; Rudall, P.J. Calcium oxalate crystals in Monocotyledons: A review of their structure and systematics. *Ann. Bot.* **1999**, *84*, 725–739. [[CrossRef](#)]
45. Solereder, H.; Meyer, F. *Systematische Anatomie der Monokotyledonen. VI. Microspermae*; Gebrüder Borntraeger: Berlin, Germany, 1930.

46. Tominski, P. Die Anatomie des Orchideenblattes in ihrer Abhängigkeit von Klima und Standort. Ph.D. Thesis, Universität Berlin, Berlin, Germany, 1905.
47. Sandoval-Zapotitla, E.; Terrazas, T.; Villaseñor, J. Diversity of mineral inclusions in the subtribe Oncidiinae (Orchidaceae). *Rev. Biol. Trop.* **2010**, *58*, 733–755. [[PubMed](#)]
48. Lee, Y.; Yeung, E.C.; Lee, N.; Chung, M. Embryo development in the Lady's Slipper orchid, *Paphiopedilum delenatii*, with emphasis on the ultrastructure of the suspensor. *Ann. Bot.* **2006**, *98*, 1311–1319. [[CrossRef](#)] [[PubMed](#)]
49. Lee, Y.; Yeung, E.C. The osmotic property and fluorescent tracer movement of developing orchid embryos of *Phaius tankervilleae* (Aiton) Bl. *Sex. Plant Reprod.* **2010**, *23*, 337–341. [[CrossRef](#)] [[PubMed](#)]
50. Yeung, E.C. A perspective on orchid seed and protocorm development. *Bot. Stud.* **2017**, *58*, 3. [[CrossRef](#)] [[PubMed](#)]
51. Volk, G.M.; Lynch-Holm, V.J.; Kostman, T.A.; Goss, L.J.; Franceschi, V.R. The Role of druse and raphide calcium oxalate crystals in tissue calcium regulation in *Pistia stratiotes* leaves. *Plant Biol.* **2002**, *4*, 34–45. [[CrossRef](#)]
52. Schwarze, F.W. Wood decay under the microscope. *Fungal Biol. Rev.* **2007**, *21*, 133–170. [[CrossRef](#)]
53. Gadd, G.M.; Bahri-Esfahani, J.; Li, Q.; Rhee, Y.J.; Wei, Z.; Fomina, M.; Liang, X. Oxalate production by fungi: Significance in geomycology, biodeterioration and bioremediation. *Fungal Biol. Rev.* **2014**, *28*, 36–55. [[CrossRef](#)]
54. Dutton, M.V.; Evans, C.S. Oxalate production by fungi: Its role in pathogenicity and ecology in the soil environment. *Can. J. Microbiol.* **1996**, *42*, 881–895. [[CrossRef](#)]
55. Lundell, T.K.; Mäkelä, M.R.; Hildén, K. Lignin-modifying enzymes in filamentous basidiomycetes—ecological, functional and phylogenetic review. *J. Basic Microbiol.* **2010**, *50*, 5–20. [[CrossRef](#)] [[PubMed](#)]
56. Andlar, M.; Rezić, T.; Marđetko, N.; Kracher, D.; Ludwig, R.; Šantek, B. Lignocellulose degradation: An overview of fungi and fungal enzymes involved in lignocellulose degradation. *Eng. Life Sci.* **2018**, *18*, 768–778. [[CrossRef](#)]
57. Peterson, R.L.; Currah, R.S. Synthesis of mycorrhizae between protocorms of *Goodyera repens* (Orchidaceae) and *Ceratobasidium cereale*. *Can. J. Bot.* **1990**, *68*, 1117–1125. [[CrossRef](#)]
58. Richardson, K.A.; Peterson, R.L.; Currah, R.S. Seed reserves and early symbiotic protocorm development of *Platanthera hyperborea* (Orchidaceae). *Can. J. Bot.* **1992**, *70*, 291–300. [[CrossRef](#)]
59. Wright, M.; Guest, D. Development of mycorrhizal associations in *Caladenia tentaculata*. *Selbyana* **2004**, *25*, 114–124.
60. Rasmussen, H.N.; Rasmussen, F.N. Orchid mycorrhiza: Implications of a mycophagous life style. *Oikos* **2009**, *118*, 334–345. [[CrossRef](#)]
61. Barsberg, S.; Lee, Y.; Rasmussen, H. Development of C-lignin with G/S-lignin and lipids in orchid seed coats—An unexpected diversity exposed by ATR-FT-IR spectroscopy. *Seed Sci. Res.* **2018**, *28*, 41–51. [[CrossRef](#)]
62. Perotto, S.; Rodda, M.; Benetti, A.; Sillo, F.; Ercole, E.; Rodda, M.; Girlanda, M.; Murat, C.; Balestrini, R. Gene expression in mycorrhizal orchid protocorms suggests a friendly plant–fungus relationship. *Planta* **2014**, *239*, 1337–1349. [[CrossRef](#)]
63. Fochi, V.; Chitarra, W.; Kohler, A.; Voyron, S.; Singan, V.R.; Lindquist, E.A.; Barry, K.B.; Girlanda, M.; Grigoriev, I.V.; Martin, F.; et al. Fungal and plant gene expression in the *Tulasnella calospora*–*Serapias vomeracea* symbiosis provides clues about nitrogen pathways in orchid mycorrhizas. *New Phytol.* **2017**, *213*, 365–379. [[CrossRef](#)]
64. Miura, C.; Saisho, M.; Yagame, T.; Yamato, M.; Kaminaka, H. *Bletilla striata* (Orchidaceae) seed coat restricts the invasion of fungal hyphae at the initial stage of fungal colonization. *Plants* **2019**, *8*, 280. [[CrossRef](#)] [[PubMed](#)]
65. Paiva, E.A.S. Are calcium oxalate crystals a dynamic calcium store in plants? *New Phytol.* **2019**, *223*, 1707–1711. [[CrossRef](#)] [[PubMed](#)]
66. Stern, W.L. *Anatomy of Monocotyledons. Volume X: Orchidaceae*; Gregory, M., Cutler, D.F., Eds.; Oxford University Press: Oxford, UK, 2014; p. 288.
67. Stern, W.L.; Carlswald, B.S. Comparative vegetative anatomy and systematics of Laeliinae (Orchidaceae). *Bot. J. Linn. Soc.* **2009**, *160*, 21–41. [[CrossRef](#)]
68. Tooulakou, G.; Giannopoulos, A.; Nikolopoulos, D.; Bresta, P.; Dotsika, E.; Orkoula, M.G.; Kontoyannis, C.G.; Fasseas, C.; Liakopoulos, G.; Klapa, M.I.; et al. Alarm photosynthesis: Calcium oxalate crystals as an internal CO₂ source in plants. *Plant Physiol.* **2016**, *171*, 2577–2585. [[CrossRef](#)] [[PubMed](#)]
69. Tulyananda, T.; Nilsen, E.T. The role of idioblasts in leaf water relations of tropical *Rhododendron*. *Am. J. Bot.* **2017**, *104*, 828–839. [[CrossRef](#)]
70. Konno, K.; Inoue, T.A.; Nakamura, M. Synergistic defensive function of raphides and protease through the needle effect. *PLoS ONE* **2014**, *9*, e91341. [[CrossRef](#)]
71. Nurfadilah, S.; Yulia, N.D.; Ariyanti, E.E. Morphology, anatomy, and mycorrhizal fungi colonization in roots of epiphytic orchids of Sempu Island, East Java, Indonesia. *Biodiversitas* **2016**, *17*, 592–603. [[CrossRef](#)]
72. Chomiccki, G.; Bidel, L.; Ming, F.; Coiro, M.; Zhang, X.; Wang, Y.; Baissac, Y.; Jay-Allemand, C.; Renner, S. The velamen protects photosynthetic orchid roots against UV-B damage, and a large dated phylogeny implies multiple gains and losses of this function during the Cenozoic. *New Phytol.* **2015**, *205*, 1330–1341. [[CrossRef](#)]
73. Muthukumar, T.; Kowsalya, A. Comparative anatomy of aerial and substrate roots of *Acampe praemorsa* (Rox.) Blatt. & MC. *Cann. Flora* **2017**, *266*, 17–28.
74. Idris, N.; Collings, D. Cell wall development in the velamen layer of the orchid *Miltoniopsis* investigated by confocal microscopy. *Malays. J. Microsc.* **2015**, *10*, 20–26.

75. Peterson, C.A.; Enstone, D.E. Functions of passage cells in the endodermis and exodermis of roots. *Physiol. Plant.* **2006**, *97*, 592–598. [[CrossRef](#)]
76. Senthilkumar, S.; Krishnamurthy, K.V.; Britto, S.J.; Arockiasamy, D.I. Visualization of orchid mycorrhizal fungal structures with fluorescence dye using epifluorescence microscopy. *Curr. Sci.* **2000**, *79*, 1527–1528.
77. Porembski, S.; Barthlott, W. Velamen radicum micromorphology and classification of Orchidaceae. *Nord. J. Bot.* **1988**, *8*, 117–137. [[CrossRef](#)]
78. Kedrowski, H.R.; Sajo, M.D.G. What are tilosomes? An update and new perspectives. *Acta Bot. Bras.* **2019**, *33*, 106–115. [[CrossRef](#)]
79. Benzing, D.H.; Ott, D.W.; Friedman, W.E. Roots of *Sobralia macrantha* (Orchidaceae): Structure and Function of the Velamen-Exodermis Complex. *Am. J. Bot.* **1982**, *69*, 608–614. [[CrossRef](#)]
80. Kwok-ki, H.; Hock-Hin, Y.; Hew, C. The presence of photosynthetic machinery in aerial roots of leafy orchids. *Plant Cell Physiol.* **1983**, *24*, 1317–1321.
81. Scarpella, E.; Meijer, A.H. Pattern formation in the vascular system of monocot and dicot plant species. *New Phytol.* **2004**, *164*, 209–242. [[CrossRef](#)] [[PubMed](#)]
82. Carlswald, B.S.; Stern, W.L.; Bytebier, B. Comparative vegetative anatomy and systematics of the angraecoids (Vandaeae, Orchidaceae) with an emphasis on the leafless habit. *Bot. J. Linn. Soc.* **2006**, *151*, 165–218. [[CrossRef](#)]
83. Moreira, A.S.F.P.; Filho, J.P.D.L.; Isaias, R.M.D.S. Structural adaptations of two sympatric epiphytic orchids (Orchidaceae) to a cloudy forest environment in rocky outcrops of Southeast Brazil. *Rev. Bio. Trop.* **2013**, *61*, 1053–1065.
84. Guan, Z.J.; Zhang, S.B.; Guan, K.Y.; Li, S.Y.; Hong, H. Leaf anatomical structure of *Paphiopedilum* and *Cypripedium* and their adaptive significance. *J. Plant Res.* **2011**, *124*, 289–298. [[CrossRef](#)]
85. Rindyastuti, R.; Nurfadilah, S.; Rahadianoro, A.; Hapsari, L.; Abywijaya, I. Leaf anatomical characters of four epiphytic orchids of Sempu Island, East Java, Indonesia: The importance in identification and ecological adaptation. *Biodiversitas* **2018**, *19*, 1906–1918. [[CrossRef](#)]
86. Roth-Nebelsick, A.; Uhl, D.; Mosbrugger, V.; Kerp, H. Evolution and function of leaf venation architecture: A review. *Ann. Bot.* **2011**, *87*, 553–566. [[CrossRef](#)]
87. Zanenga-Godoy, R.; Costa Gonçalves, C. Foliar anatomy of four species of genus *Cattleya* Lindl. (Orchidaceae) of the Brazilian Central Planalt. *Acta Bot. Bras.* **2003**, *17*, 101–118. [[CrossRef](#)]